



Using Longitudinal Stiffeners to Mitigate Buckling of Noncompact and Slender Beam Webs in Ductile Moment Frame Connections

Matthew R. Eatherton¹, Yujia Chen², Karim Laknejadi³, Thomas M. Murray⁴

Abstract

Typical beam sections used in metal buildings have noncompact or slender webs. It is often difficult, therefore, for these economically designed deep built-up members to meet highly ductile or moderately ductile web slenderness (h/t_w) requirements in the AISC *Seismic Provisions* for use in special or intermediate moment resisting frame connections. A combined experimental and computational research program has been conducted to investigate a design strategy whereby longitudinal web stiffeners are used to break the web into panels which individually satisfy ductile slenderness requirements. Full-scale cyclic tests on three 1219 mm (48 in.) deep end plate moment connection subassembly specimens demonstrate the effectiveness of this design strategy. A computational study using finite element models validated against the full-scale experiments is used to extend the applicability of the results. It is shown that moment connections with longitudinal stiffeners can develop substantial ductility and satisfy qualification requirements for special moment resisting frame connections even if the beam web outside the connection region is noncompact or slender.

1. Introduction

Typical built-up sections for metal buildings have relatively thin webs compared to rolled I-sections. The web slenderness (h / t_w) for deep built-up members can be considerably larger than the limits for highly ductile members or moderately ductile members as specified in the AISC *Seismic Provisions* (AISC 2010a). However, previous tests suggest that with proper detailing, these members may be able to develop adequate cyclic performance (Ryan and Murray 1999) for use in ductile moment frames. The goal of this paper is to develop a strategy for stiffening the moment connection region of a noncompact-web or slender-web beam to produce sufficient ductility and inelastic rotation to satisfy special moment resisting frame (SMRF) criteria.

¹ Associate Professor, Virginia Tech, <meather@vt.edu>

² Graduate Research Assistant, Virginia Tech, <cyujia@vt.edu>

³ Graduate Research Assistant, Iran University of Science and Technology, <k.laknejadi@gmail.com>

⁴ Emeritus Professor, Virginia Tech, <thmurray@vt.edu>

The *Specification* (AISC 2010b) includes criteria for evaluating whether the web or flange of an I-shaped section is compact, noncompact or slender. Criteria in a similar form are provided in the *Seismic Provisions* (AISC 2016a) to determine whether a section is considered highly ductile (capable of 0.04 rad of rotation) or moderately ductile (capable of 0.02 rad of rotation). In both references, the criteria are based on separately evaluating the slenderness of the flange and web. This separate evaluation should not be interpreted to mean that the propensity for flange local buckling and web local buckling are separate. Equations for web and flange buckling presented in the literature show that the two are intimately linked (e.g. Salmon and Johnson 1996, Bleich 1952, Ziemian 2010).

Salmon and Johnson (1996) demonstrates the development of compactness criteria wherein plate buckling equations are used to evaluate buckling for the web and flange separately and the boundary conditions at the intersection of the two are assumed to be between simply supported and fixed. The assumption of how much rotational rigidity the web provides to the flange is key in the present study.

In tests on ductile moment connection subassemblages, it is often flange local buckling that is cited as causing degradation in the moment strength (e.g. Sumner and Murray 2002). One might think, therefore, that a section with a flange satisfying the highly ductile criterion might be capable of retaining significant moment strength through large rotations even if the web does not satisfy its highly ductile criterion. However, once web local buckling occurs, the amount of rotational rigidity provided by the web to the flange reduces substantially, the assumption used to develop the flange local buckling criterion is invalidated, and flange local buckling can occur. In fact, the buckled shape will likely be a combination of both web and flange local buckling, not an isolated web buckling shape.

Figure 1 describes this issue and the proposed solution. For a section such as the one shown in Figure 1a, the highly ductile limit for flange slenderness, λ_{f-hd} , assumes a certain level of rotational restraint provided by the web. If the web slenderness, λ_w , is larger than the highly ductile limit for web slenderness λ_{f-hd} , given in the *Seismic Provisions* Table D1.1 (AISC 2010a), the flange may experience flange local buckling as the web buckles. The proposed solution is to increase the rotational restraint the web provides to the flange by adding longitudinal beam web stiffeners in the connection region. Guidance for the use of longitudinal beam web stiffeners can be found in references such as Bleich (1952) and bridge design procedures (AASHTO 2016).

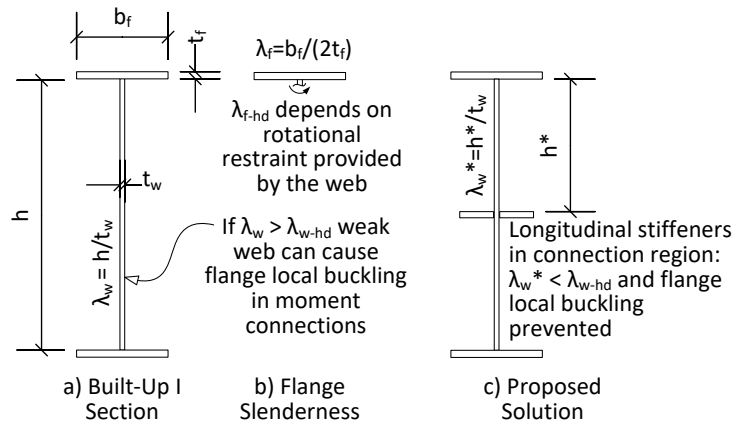


Figure 1: Description of Problem and Proposed Solution

A combined experimental and computational study was conducted to investigate whether longitudinal beam web stiffeners are capable of producing ductile SMRF type of behavior in moment connections with noncompact and slender web beams. Three moment connections (unstiffened, transverse stiffener, longitudinal stiffeners) were tested, all with noncompact webs and flanges within the highly ductile limit. The companion computational study examined the cyclic buckling behavior of a set of 16 additional configurations.

2. Proposed Solution

The proposed solution is to add longitudinal stiffeners until the effective web height, h^* , defined as the clear distance between longitudinal stiffeners or between longitudinal stiffeners and the flange, results in an effective web slenderness, λ_w^* as given in Eq. 1 that is less than the highly ductile limits in the *Seismic Provisions* (AISC 2010a). It is advantageous to locate the stiffeners as close to mid-depth as possible to have the least effect on plastic moment strength of the beam.

$$\lambda_w^* = \frac{h^*}{t_w} \quad (1)$$

As demonstrated in Figure 2, the stiffeners should extend from the moment connection to the point where the design moment strength of the unstiffened beam including local web buckling strength reductions as applicable (e.g. ϕMn for LRFD) is greater than the required moment strength. The required moment strength can be determined from the moment diagram assuming that the moment at the plastic hinge is equal to the expected strain hardened moment capacity, M_{pr} , as defined in AISC 358 (AISC 2016).

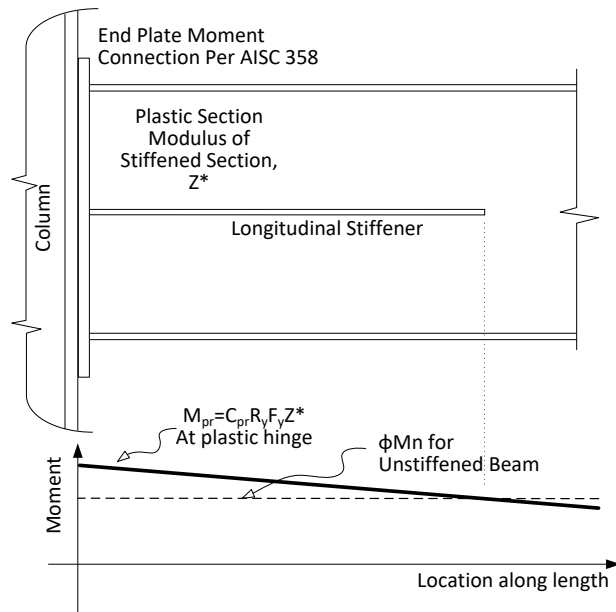


Figure 2: Length of Longitudinal Stiffeners

There are several sources of guidance for detailing the width, thickness, and welding of the longitudinal stiffeners. Bleich (1952) derives the required moment of inertia of longitudinal stiffeners for a single pair of stiffeners at mid-depth and two pairs of stiffeners equidistant across the web height that are required so that the web plate on either side of the stiffener buckles as a simply supported plate (assuming uniform compression in the plate, not bending). Alternatively, AASHTO gives requirements for width, moment of inertia, and radius of gyration for longitudinal stiffeners as shown in Eq. 2 to Eq. 4 (AASHTO 2016).

$$b_s \leq 0.48 t_s \sqrt{\frac{E}{F_{ys}}} \quad (2)$$

$$I_s \geq h_w t_w^3 \left[2.4 \left(\frac{d_o}{h_w} \right)^2 - 0.13 \right] \beta \quad (3)$$

$$r_s \geq \frac{0.16 d_o \sqrt{\frac{F_{ys}}{E}}}{\sqrt{1 - 0.6 \frac{F_{yc}}{R_h F_{ys}}}} \quad (3)$$

The stiffener has width, b_s , thickness, t_s , modulus of elasticity, E , and yield stress, F_{ys} . The web height, h_w , and thickness, t_w , was defined in Figure 1. The distance between centerline of the longitudinal stiffener and the flange is d_o , the factor β is a curvature correction factor and can be taken as 1.0 for straight webs. The radius of gyration of the longitudinal stiffener, r_s , is calculated including an effective width of web equal to $18t_w$. The factor R_h is a hybrid factor that can be taken equal to 1.0 and F_{yc} is the yield stress of the compression flange.

3. Experimental Program

3.1 Test Specimens

A set of three subassembly moment connection tests (see Table 1) were performed at the Thomas M. Murray Structural Engineering Laboratory at Virginia Tech to investigate the use of longitudinal stiffeners in moment connections. As shown in Figure 3, all specimens had a depth, $d = 1219\text{mm}$, flange width, $b_f = 152\text{ mm}$, flange thickness, $t_f = 13\text{ mm}$, and web thickness, $t_w = 9.5\text{ mm}$. The flange slenderness and web slenderness are $\lambda_f = b_f / (2 t_f) = 6$ and $\lambda_w = h_w / t_w = 125$, respectively. For ASTM A529 Gr. 55 steel with zero compression force, the highly ductile limits for the flange and web are $\lambda_{f-hd} = 6.9$ and $\lambda_{w-hd} = 56$, respectively. The flange, therefore satisfies the highly ductile criterion, while the web has a slenderness that is more than twice the highly ductile limit.

Table 1: Test Matrix

Specimen Number	Beam Web Stiffeners	M_p at end (kN-m)	M_p^* with stiffeners (kN-m)
1	None	2170	-
2	Transverse	2170	-
3	Longitudinal	-	2380

The specimen detailing is shown in Figure 3. Specimen 1 did not have any stiffeners and served as a benchmark to evaluate improvement in behavior due to stiffeners. Specimen 2 had a single pair of transverse stiffeners located 686 mm from the face of the column. The transverse stiffeners were expected to act to restrict web buckling. Specimen 3 as shown in Figure 3c had two pairs of longitudinal stiffeners. The effective web height between the longitudinal stiffeners and the flange is $h^*=438$ mm leading to an effective web slenderness, $h_w / t_w = 46$ which is within the highly ductile limits (i.e. less than $\lambda_{w-hd} = 56$).

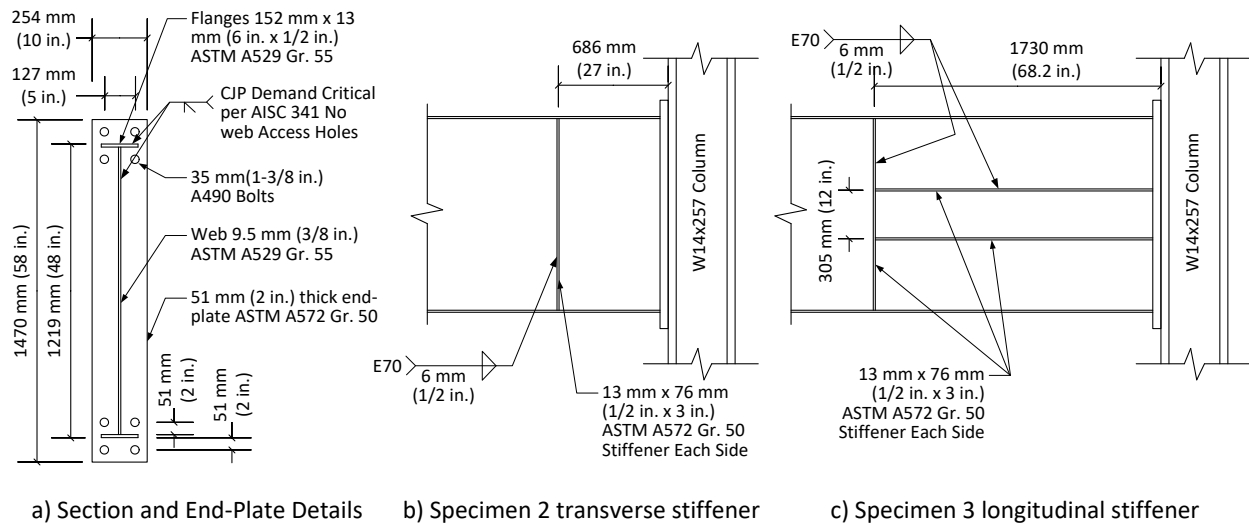


Figure 3: Test Specimen Geometry

3.2 Experimental Setup

The test setup is shown in Figure 4. A single-sided beam configuration was used and the W14x257 column was reused for all specimens. Specimen 1 and Specimen 3 were part of the same physical beam. The beam was turned around and flipped over between the tests. The subassembly was subjected to cyclic story drift through displacement control of the end of the beam at the location of the actuator. The specimens were subjected to the cyclic loading protocol outlined in Chapter K of the *Seismic Provisions* for SMRF qualification testing (AISC 2010a).

The bolts at the end-plates were fully pretensioned using the turn-of-the-nut method. A suite of instrumentation was used, but the measurements reported in this paper came from the actuator load cell and a string potentiometer immediately under the actuator measuring beam displacement. The displacements of the top and bottom of the column were recorded, but found to be negligible. Approximate locations of lateral bracing are shown in Figure 4, but for some tests, there was an excessive gap between the sides of the beam and the lateral bracing as discussed below in the results.

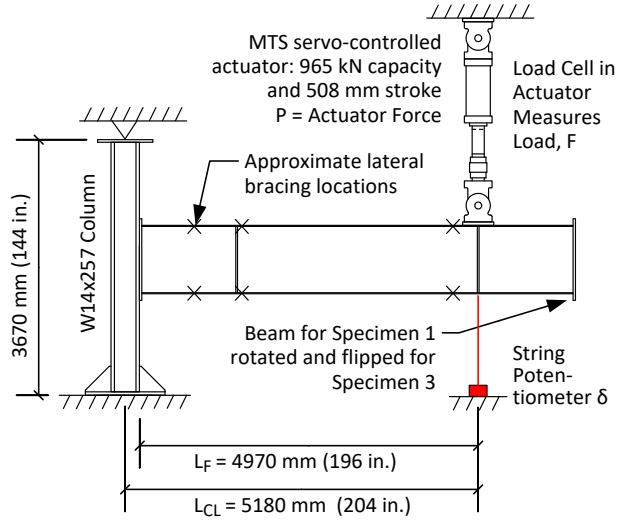


Figure 4: Test Specimen Geometry

3.3 Material Tests

Eight coupons were subjected to uniaxial monotonic tension to obtain material properties. Coupons were cut from portions of the beam flanges and webs located outside the plastic hinge region after subassembly testing. Material tests were conducted in accordance with ASTM E8 (ASTM 2016) with a 203 mm gage length and 38 mm width. Figure 5 shows a representative stress-strain behavior from one of the coupon tests and Table 2 gives the measured yield stress, ultimate stress, and elongation from the tests. A 51 mm. gage length extensometer was used to measure strain at the beginning of the test, but had to be removed at a strain below 0.05 m/m due to limited displacement range. Strains above this value were calculated as crosshead displacement divided by an effective length.

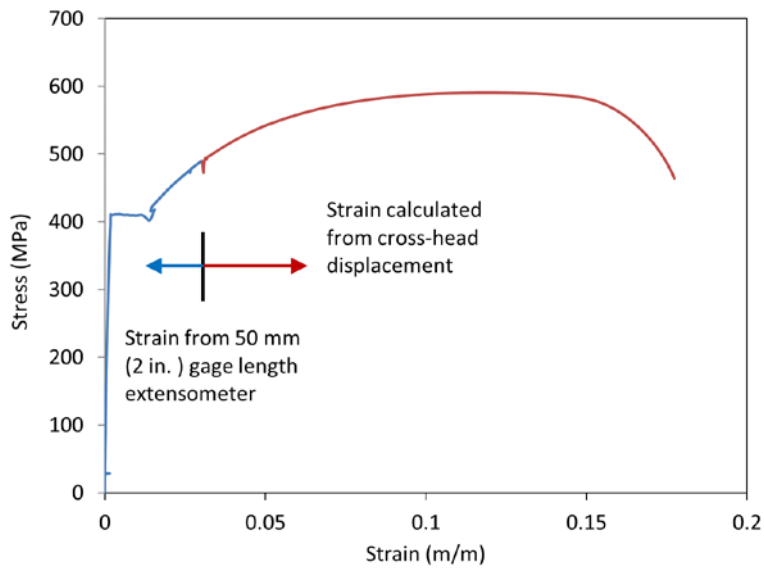


Figure 5: Example Material Test Results (from Specimen 3 Flange)

Table 2: Measured Material Properties

Specimen Number	Location	Number of Specimens	Yield Stress (MPa)	Ultimate Stress (MPa)	Elongation (m/m)
1 & 3	Flange	2	410	587	0.177
1 & 3	Web	1	390	478	0.179
2	Flange	3	401	580	0.188
2	Web	2	436	570	0.185

3.4 Results

The moment vs. story drift responses of the three specimens are shown in Figure 6. Moment is calculated as the force multiplied by the distance to the face of the column. Story drift is calculated as the measured beam displacement at the actuator location divided by the distance between the actuator and the centerline of the column.

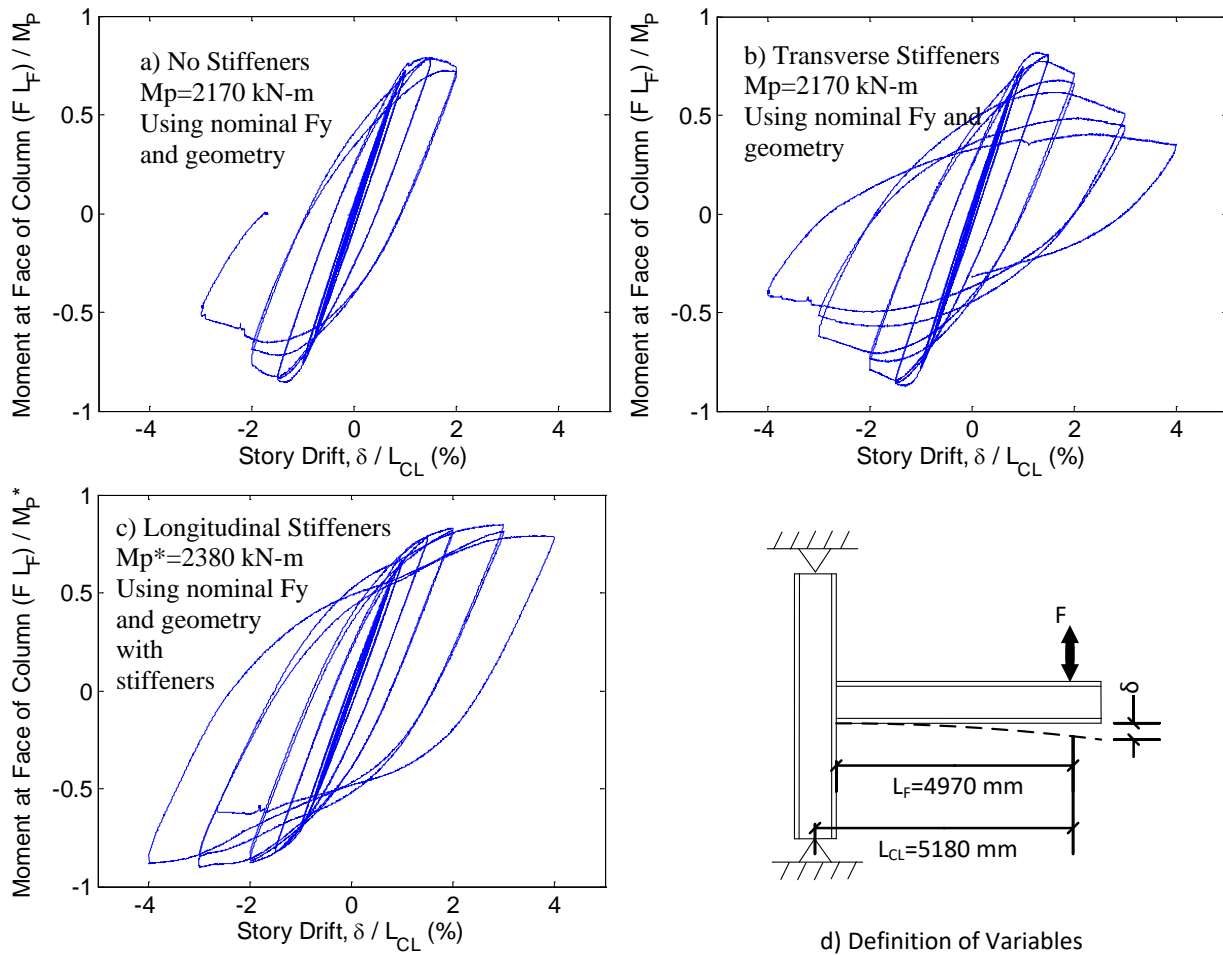


Figure 6: Results from Experimental Program

Specimen 1 experienced buckling starting in the cycles at 1.5% story drift and worsening through the 2% cycles. During the first cycle at 3% story drift the test was stopped due to excessive deformation at the location of the lateral bracing. As shown in Figure 6a, the moment strength reached 85% of the nominal plastic moment strength, M_p , and during the beginning of the 3% story drift cycle, the moment strength had degraded to $0.5 M_p$. Figure 7 shows the buckled shape of Specimen 1. The web buckle had a long half wave that exceeded the dimension d . Flange local buckles formed at a distance from the end-plate approximately equal to the depth of the beam, d .

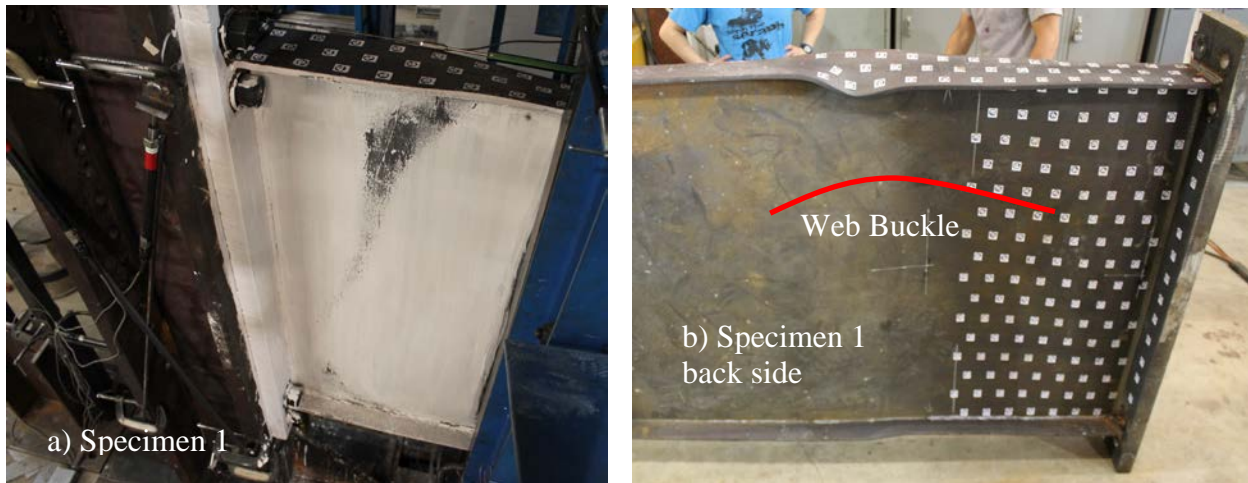


Figure 7: Picture of Specimen 1 Buckled Shape a) in test rig, and b) back side of specimen after being disassembled

Specimen 2 experienced similar strength degradation as Specimen 1, but the buckling shape was different. The entire section between the last lateral brace and the column buckled out-of-plane as shown in Figure 8a.

Specimen 3 exhibited more full hysteresis loops as shown in Figure 6c. The specimen resisted a maximum moment approximately equal to 90% of the nominal moment capacity calculated including the longitudinal stiffeners, M_p^* . The lateral bracing for the specimen was erected with a gap of approximately 75 mm between the sides of the beam and the lateral support. As a result, the beam was effectively not laterally braced at the plastic hinge. The beam underwent lateral torsional buckling as shown in Figure 8c. Local buckles were observed in the flanges near the end plate as shown in Figure 8b. During the 4% story drift cycle, the weld between the web and flange started to fracture and unzip. The test was halted after significant unzipping occurred.

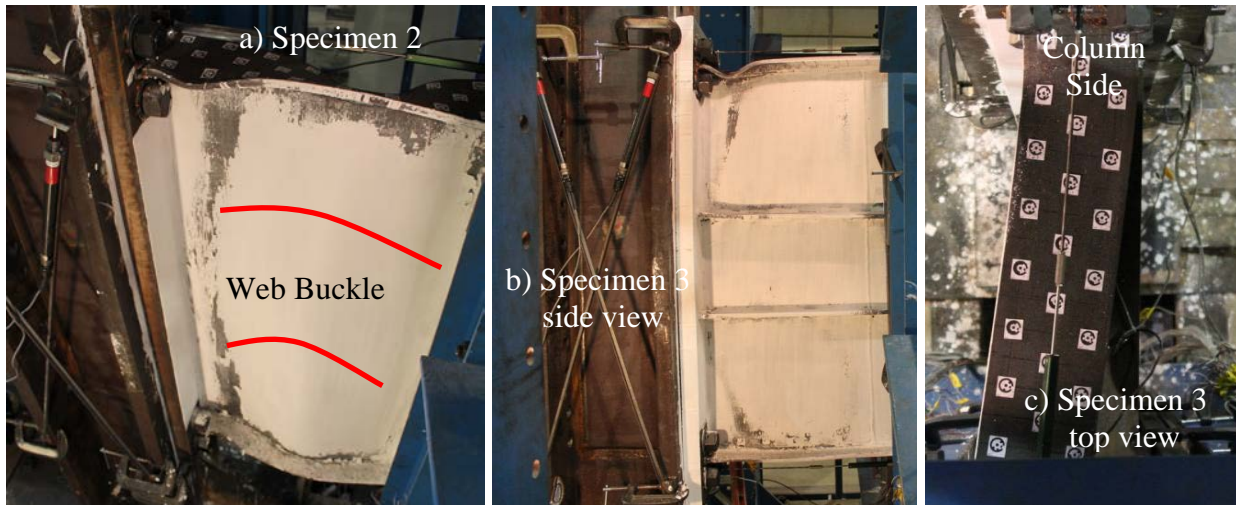


Figure 8: Picture of Specimen 2 and 3 buckled shape

3.5 Summary

The failure mode of Specimen 1 demonstrates that this beam with a noncompact web was unable to develop a plastic hinge because web buckling led to flange buckling and associated moment strength degradation. Specimen 2 showed that transverse stiffeners broke up the web panel, but was unable to prevent web and flange buckling between the transverse stiffeners and the end-plate. A finite element study, not shown here, found that a series of transverse stiffeners spaced every 200 mm was incapable of preventing flange local buckling because the flange local buckles have a relatively short half wave length that can fit between transverse stiffeners.

Specimen 3 demonstrated the potential of the longitudinal stiffener concept even if the specimen itself was subject to limit states unrelated to flange local buckling. Although the resulting behavior did not reach the full nominal plastic moment strength, M_p^* , of the stiffened section, the moment strength did not degrade substantially until the beam flange started to separate from the beam web. It is expected that both lateral torsional buckling and weld fracture at the beam web to flange would have been prevented if the requirements of AISC 358 (AISC 2016) were followed. The weld between the flange and web was a single-sided fillet weld whereas AISC 358 requires a double sided fillet weld in the connection region. Considering these limitations of Specimen 3, it is concluded that the longitudinal stiffener concept, although not fully proven by this test, is shown to have great potential for limiting flange local buckling and thus achieving special moment frame connection behavior.

4. Computational Study

A computational study was conducted to further investigate the use of longitudinal web stiffeners in the beam moment connection region to mitigate flange local buckling and thus develop ductile SMRF type of behavior. First, the computational modelling approach is described and the load-deformation response is validated against experimental data. Next, an example beam section is described along with the application of the proposed longitudinal stiffeners and the resulting improvement in moment vs. story drift response. Finally, a set of sixteen configurations that

have noncompact and slender webs are investigated to determine if longitudinal stiffeners can prevent local buckling in these moment connection configurations.

4.1 Computational Modelling Approach and Validation

Computational models such as the one shown graphically in Figure 9b were created using four node reduced integration shell elements in the ABAQUS software (Dessault Systemes 2016). A mesh size of 25 mm was used in the connection region and a mesh size of 50 mm was used outside of the connection region. The results were compared to the results from a mesh size half that size (not shown here), and the moments were found to be within approximately 5% of one another. The Armstrong-Frederick plasticity model was used which has combined nonlinear isotropic and kinematic hardening. The plasticity model was calibrated to have the same nonlinear stress-strain behavior as the experimental tension coupons described above.

Figure 9 shows a comparison between the behavior of Specimen 2 and the computational model of Specimen 2. The shape and size of the flange and web buckles were captured well. Both exhibited approximately 2 half waves in the top and bottom flanges and a web buckling deformation mode wherein the entire web buckled in one direction making a vertical crease. The computational moment versus story drift response tracked the experimental curve as shown in Figure 9c and the cumulative energy was within 6% of the experiment at the end of the loading protocol (Figure 9d).

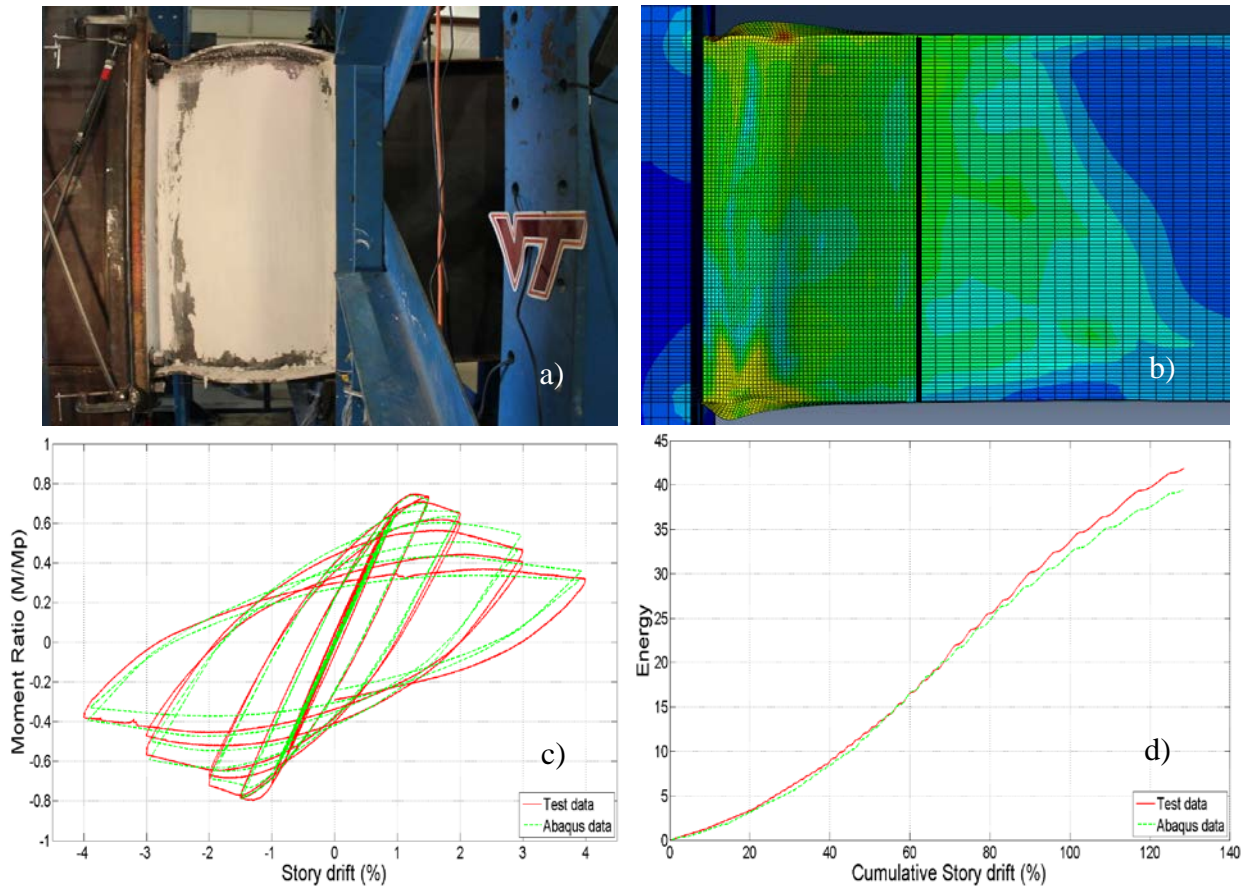


Figure 9: Validating Computational Model Against Results of Specimen 2 with Transverse Stiffener

4.2 Example Application of Longitudinal Stiffeners

An example application of longitudinal stiffeners is shown in Figure 10. The beam has depth, $d = 1220$ mm, flange width, $b_f = 305$ mm, flange thickness, $t_f = 30.5$ mm, and web thickness, $t_w = 7.6$ mm. The resulting flange slenderness and web slenderness are, $\lambda_f = 5$ and $\lambda_w = 160$. The web is slender according to the *Specification* (AISC 2010b). Figure 10a shows that the beam undergoes significant web buckling during cyclic loading and is incapable of developing the plastic moment capacity.

Two pairs of web stiffeners were added in the connection region as shown in Figure 10b to mitigate web buckling. The stiffeners were sized according to the AASHTO rules described above which resulted in stiffeners that are 9.5 mm x 72 mm (0.375 in. x 2.85 in.). Figure 10b shows the deformed shape of the model during the 4% story drift cycles. It is shown that web buckling is greatly reduced, plastic hinges form, and local flange buckles occur at large story drift angles. Figure 11 shows that the configuration with longitudinal stiffeners is capable of large inelastic deformations with negligible moment strength degradation. During the 4% story drift cycles, the peak moment of the configuration with longitudinal stiffeners and without are 7790 kN-m (5748 k-ft) and 3870 kN-m (2857 k-ft) respectively. This corresponds to 1.04 and 0.65 times the nominal plastic moment strength of the sections, respectively. Adding longitudinal stiffeners led to approximately twice the moment strength at 4% drift and satisfies the AISC 341 qualification criterion for SMRF connections (moment strength of at least $0.8M_p$ at 4% story drift).

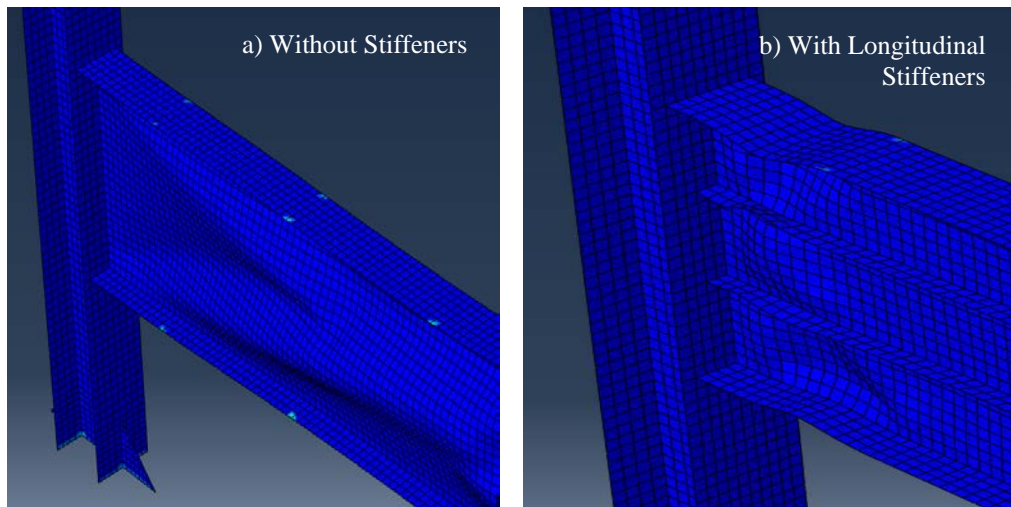


Figure 10: Deformed Shape for Example Application of Longitudinal Stiffeners

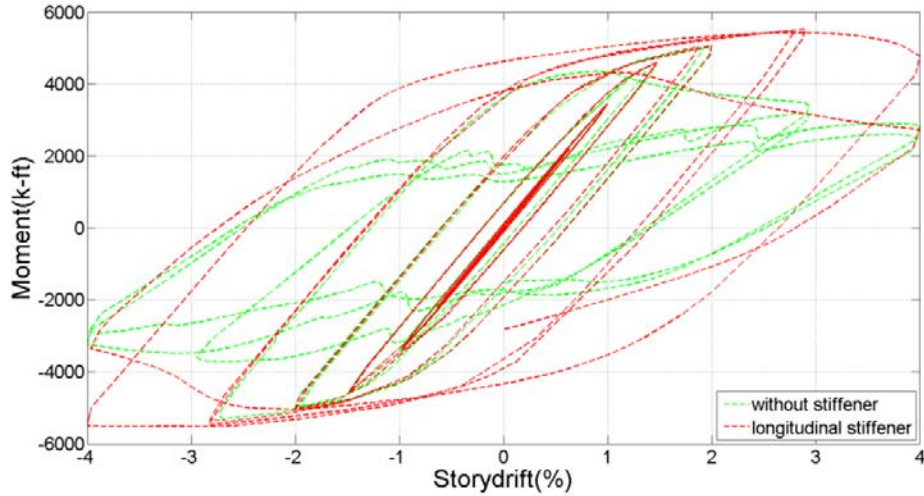


Figure 11: Results from Example Application of Longitudinal Stiffeners

4.3 Study of a Range of Configurations

Additional configurations were investigated with the computational modeling approach described in the previous sections. Sixteen configurations were simulated as detailed in Table 3. The ratio of moment strength during the 4% story drift cycle to the nominal plastic moment strength is given for configurations with and without longitudinal stiffeners. Cells that are shaded in the table represent configurations that satisfied the SMRF qualification criteria specified in the *Seismic Provisions* (AISC 2010a). Interestingly, the configurations with lower web slenderness passed the qualification criteria without longitudinal stiffeners. This result suggests there is some conservatism in the highly ductile web slenderness limits.

Table 3: Summary of FE Model Results (shaded cells indicate not meeting SMRF qualification)

d mm	b _f mm	t _f mm	t _w mm	$\frac{b_f}{2t_f}$	$\frac{h}{t_w}$	No Stiffeners		With Longitudinal Stiffeners			
						M _p kN-m	$\frac{M_{4\%}}{M_p}$	No. of Stiffeners	$\frac{h_w^*}{t_w}$	M _p * kN-m	$\frac{M_{4\%}}{M_p^*}$
1220	305	22.9	7.6	6.67	160	4752	0.63	2	53.3	5895	0.89
1220	305	22.9	10.2	6.67	120	5143	0.93	1	60	5159	1.08
1220	305	25.4	7.6	6	160	5158	0.65	2	53.3	6427	0.95
1220	305	25.4	10.2	6	120	5549	0.91	1	60	5568	1.31
1220	305	30.5	7.6	5	160	5975	0.65	2	53.3	7498	1.04
1220	305	30.5	10.2	5	120	6366	1.12	1	60	6394	1.26
1220	305	31.8	7.6	4.8	160	6180	0.67	2	53.3	7767	1.02
1220	305	31.8	10.2	4.8	120	6571	1.16	1	60	6602	1.23
813	203	15.2	5.1	6.67	160	1408	0.38	2	53	2666	0.76
813	203	15.2	6.8	6.67	120	1524	0.88	1	60	2324	0.88
813	203	16.9	5.1	6	160	1529	0.36	2	53	1725	1.21
813	203	16.9	6.8	6	120	1645	1.09	1	60	1586	1.40
813	203	20.3	5.1	5	160	1770	0.51	2	53	2193	1.29
813	203	20.3	6.8	5	120	1887	1.01	1	60	1952	1.30
813	203	21.2	5.1	4.8	160	1831	0.59	2	53	2271	1.29
813	203	21.2	6.8	4.8	120	1947	1.02	1	60	2013	1.29

Table 3 and Figure 12 show the effect of adding longitudinal web stiffeners. After adding either one or two pairs of longitudinal stiffeners, the effective web slenderness, $\lambda_w^* = h_w^* / t_w$ was near or below the limit for highly ductile members (calculated assuming no compression force). All except one of the stiffened sections retained 80% of their nominal plastic moment strength after being subjected to the AISC 341 Chapter K loading protocol through 4% story drift. This demonstrates the advantages of the longitudinal stiffener approach for reinforcing moment connection regions with noncompact or slender webs.

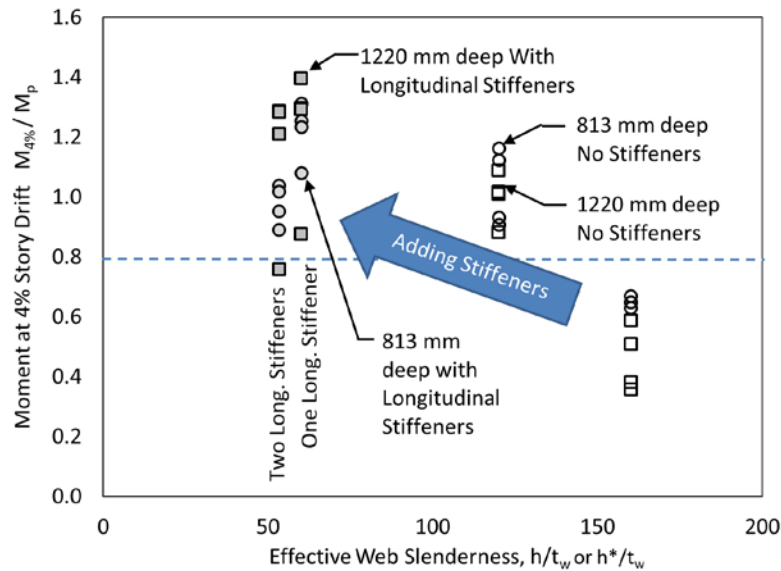


Figure 12: Summary of the Effect of Longitudinal Stiffeners on Moment at 4% Story Drift

5. Conclusions

Current methods for evaluating slenderness of elements of a cross section in the AISC *Specification* and AISC *Seismic Provisions* evaluates the flange and web of an I-shaped section separately. Since the flange local buckling criterion depends on a certain amount of rotational rigidity from the web, a noncompact or slender web can lead to flange local buckling in moment connections. A solution was proposed wherein longitudinal stiffeners are used in the connection region to mitigate web buckling and increase the rotational stiffness provided to the flange by the web.

A combined experimental and computational study was conducted to explore the use of longitudinal stiffeners to mitigate web buckling and flange local buckling in moment connections with beams having noncompact or slender webs. Three full-scale moment connection subassembly specimens were tested including one specimen each with no stiffeners, transverse stiffeners and longitudinal stiffeners. The specimen with transverse stiffeners experienced flange and web buckling that caused moment strength degradation similar to the specimen without any stiffeners. On the other hand, the specimen with longitudinal stiffeners exhibited small moment strength degradation and stable hysteretic behavior up to the 4% story drift cycles.

A computational modeling approach was validated against test data and was found to capture the relevant buckling modes. Sixteen moment connection configurations were computationally investigated. It was found that almost all of the configurations with longitudinal stiffeners were able to satisfy qualification criteria for special moment resisting frames.

The combined experimental and computational study proved that longitudinal stiffeners can substantially improve moment connection ductility and is a promising approach for mitigating web and flange local buckling in moment connections that use beams having noncompact or slender webs. More testing and simulation is warranted to further verify the behavior for a wider range of configurations and further develop and validate detailing rules.

Acknowledgments

NUCOR Building Systems donated all the specimens tested in this study. Thanks to Scott Russel, American Building Company and NUCOR Building Systems. The authors appreciate the work of Brad Toellner and Charles Watkins who helped conduct the full scale tests.

References

- AASHTO (2016) "AASHTO LRFD Bridge Design Specifications" 7th Edition with 2015 and 2016 Interim Revisions
- AISC (2010a) "ANSI/AISC 341-10 Seismic Provisions for Structural Steel Buildings" Published by the American Institute of Steel Construction
- AISC (2010b) "ANSI/AISC 360-10 Specification for Structural Steel Buildings" Published by the American Institute of Steel Construction
- AISC (2016) "ANSI/AISC 358-16 Prequalified Connections for Special and Intermediate Steel Moment Frames for Seismic Applications" Published by the American Institute of Steel Construction
- ASTM (2016) "ASTM E8/E8M-16a Standard Test Methods for Tension Testing of Metallic Materials" American Society for Testing and Materials.
- Bleich, F. (1952) "Buckling Strength of Metal Structures" Published by McGraw-Hill Book Company
- Dassault Systemes (2016) "Abaqus Unified FEA Users Manual"
- Ryan, J.C., and Murray, T.M. (1999). "Evaluation of the Inelastic Rotation Capability of Extended End-Plate Moment Connections." *Virginia Polytechnic Institute and State University Structural Engineering and Materials Report No. CE/VPI-ST 99/13*.
- Salmon, C.G., Johnson, J.E., and Malhas, F.A. (1996) "Steel Structures Design and Behavior, Fourth Edition" Published by Prentice Hall
- Sumner E.A. and Murray, T.M. (2002) "Extended End-Plate Moment Connections Subject to Cyclic Loading" *Journal of Structural Engineering* 128 (4) pp. 501-508.
- Ziemian, R.D. (2010) "Guide to Stability Design Criteria for Metal Structures" Sixth Edition, Published by John Wiley & Sons